IEEE Photonics Journal
An IEEE Photonics Society Publication

Open Access

Flexible Solar-Blind Ga_2O_3 Ultraviolet Photodetectors With High Responsivity and Photo-to-Dark Current Ratio

Volume 11, Number 6, December 2019

Zhe Li
Yu Xu
Jiaqi Zhang
Yaolin Cheng
Dazheng Chen
Qian Feng
Shengrui Xu
Yachao Zhang
Jincheng Zhang
Yue Hao
Chunfu Zhang

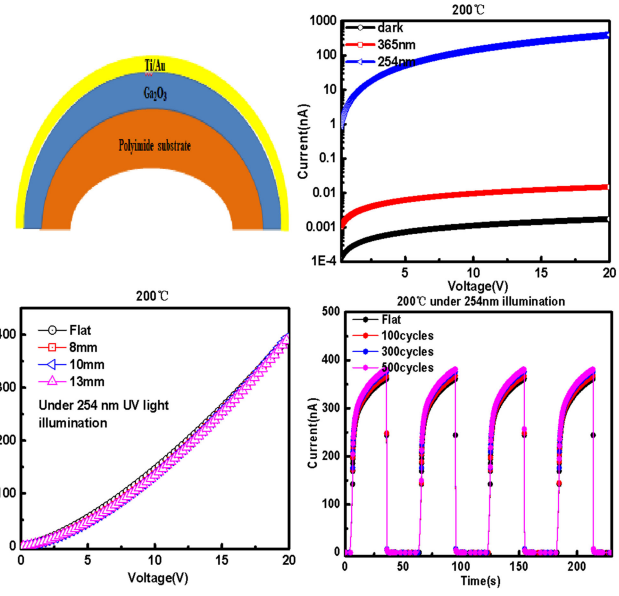

DOI: 10.1109/JPHOT.2019.2946731

Flexible Solar-Blind Ga_2O_3 Ultraviolet Photodetectors With High Responsivity and Photo-to-Dark Current Ratio

Zhe Li, Yu Xu, Jiaqi Zhang, Yaolin Cheng, Dazheng Chen, Qian Feng, Shengrui Xu, Yachao Zhang, Jincheng Zhang, Yue Hao, and Chunfu Zhang

Wide Bandgap Semiconductor Technology Disciplines State Key Laboratory, School of Microelectronics, Xidian University, Xi'an 710071, China

DOI:10.1109/JPHOT.2019.2946731

Manuscript received August 31, 2019; revised September 27, 2019; accepted October 5, 2019. Date of publication October 10, 2019; date of current version November 12, 2019. This work was supported in part by National 111 Center under Grant B12026 and in part by the National Natural Science Foundation of China under Grants 61604119 and 11435010. Corresponding author: Chunfu Zhang (e-mail: cfzhang@xidian.edu.cn).
This paper has supplementary downloadable material available at http://ieeexplore.ieee.org, provided by the authors.

Abstract: In this work, flexible solar blind Ga_2O_3 ultraviolet photodetectors with high responsivity and photo-to-dark current ratio are demonstrated. The Ga_2O_3 films are obtained by the RF magnetron sputtering method on flexible polyimide (PI) substrates and the results demonstrate that all the films grown under various temperatures are amorphous. When the incident light wavelength is less than 254 nm, the incident light is effectively absorbed by the Ga_2O_3 film. By controlling the growth temperature of the material, the responsivity and photo-to-dark current ratio of the corresponding metal-semiconductor-metal photodetectors are significantly improved. At growth temperature of 200 °C, the current under 254 nm illumination obtains 396 nA at voltage of 20 V (corresponding responsivity is 52.6 A/W), the photo-to-dark current ratio is more than 10^5, and the external quantum efficiency reaches 2.6×10^4%, which is among the best reported Ga_2O_3 ultraviolet photodetectors including the devices on the rigid substrates. After the bending and fatigue tests, the flexible detectors have negligible performance degradation, showing excellent mechanical and electrical stability.

Index Terms: Ga_2O_3, solar blind photodetector, flexible device, responsivity, photo-to-dark current ratio.

1. Introduction

In today's fast-developing information age, optoelectronic technology has become a frontier discipline in the information industry. A wide variety of optoelectronic devices, such as lasers [1], light-emitting diodes [2], photodetectors [3], [30] and solar cells [4], have penetrated into all aspects of human life and work. They also play an important role in the fields of space exploration [5] and national defense security. As one of the core components of optoelectronic devices, photodetectors play the role of converting optical signals into electrical signals in optoelectronic communication systems. In addition, photodetectors also have significant applications in military operations, acting as monitoring, detection, tracking and identifying features [6]–[9].

Due to its unique advantages of low noise and high sensitivity, the solar blind ultraviolet (UV) photodetector has become a new research hotspot in the field of photoelectric detection. In order to make the solar blind UV photodetector more widely used, the substrate material of the photodetector is particularly important. The rigid substrates such as sapphire and quartz are commonly used, but they are relatively hard, require some complicated cutting process [22]. At the same time, rigid substrates are relatively brittle, easy to break, etc; Compared to rigid substrates, flexible substrates are relatively inexpensive and easy to handle, and have broad application prospects in photodetectors; And the flexible solar blind UV photodetector is also widely integrated into the detection system because it is soft, wearable and portable [10]–[12].

Solid-state solar blind UV photodetectors are mainly developed based on semiconductor materials [26]–[29]. Although the mainstream silicon-based semiconductors in the market also have UV response, the band gap of the silicon-based material is too narrow, resulting in a high visible and infrared response. In addition, silicon-based materials have poor characteristics under high pressure and high temperature condition, which further limits their development in the field of solar blind UV detection. Therefore, the solar blind UV photodetector using a wide band gap semiconductor as the photosensitive material is currently pursuing. As a wide bandgap oxide semiconductor material, Ga_2O_3 has a quasi-direct gap of up to 4.8 eV, and its photoresponse peak falls in the solar-blind band. It does not require energy band regulation, and its absorption coefficient near the absorption edge is as high as 10^5 cm^{-1}. It is an ideal natural solar blind UV detection material [13], [14]. In addition, Ga_2O_3 materials are inexpensive, have good thermal and chemical stability, and can withstand high electric fields up to 8 MV/cm [15]–[18]. So it is stable material and can be used under severe conditions.

In this work, the Ga_2O_3 films were grown by radio frequency magnetron sputtering technique on flexible PI substrates under different growth temperatures (50–200 °C). By controlling the growth temperature, the fabricated interdigitated solar blind UV photodetectors exhibit excellent characteristics, including a large spectral responsivity (52.6 A/W), low dark current (1.7 pA at 20 V), large photo-to-dark current ratio ($>10^5$), high external quantum efficiency ($>10^4$%). At the same time, the flexible photodetectors show excellent mechanical and electrical stability.

2. Experimental Details

2.1 Materials Growth

Ga_2O_3 films were deposited on PI and sapphire substrates respectively by radio frequency magnetron sputtering at different temperatures. Ga_2O_3 ceramic target has high purity (99.99%). The PI and sapphire substrates were ultrasonically cleaned in acetone, alcohol, and deionized water. Firstly, the vacuum was evacuated to the base pressure of 1×10^{-6} Torr. The film thickness under all conditions was kept at 200 nm. And sputtering power was set to 120 W and deposited pressure was 25 mTorr. The processing atmosphere was pure argon (Ar). The argon flow rate is always 20 sccm during the entire sputtering process. The only change in growth conditions is temperature, which varied from 50 °C to 200 °C (the highest reliable temperature for our PI substrates).

2.2 Photodetectors Fabrication

The Ga_2O_3 solar-blind UV photodetector were constructed with a MSM interdigitated structure through standard lithography and lift-off procedures. Each of electrode fingers is 80 μm long and 3 μm wide. It is 3 μm wide between two fingers (As shown in Fig. 1).

2.3 Characterizations

Optical transmittance was characterized by Dual-beam UV-Vis spectrometer (Perkin-Elmer Lambda 950). The crystal structure of the film is illustrated by the X-ray diffractometer (D8 Advance, Bruker, Germany). The elemental composition was studied by X-ray photoelectron spectroscopy using ESCALAB 250Xi spectrometer. The surface morphologies were analyzed using a field effect scanning

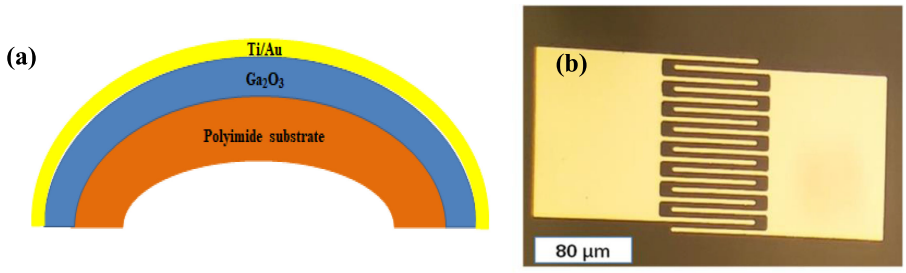

Fig. 1. (a) Schematic cross section and (b) top view of the fabricated Ga_2O_3 thin film MSM structure flexible photodetector.

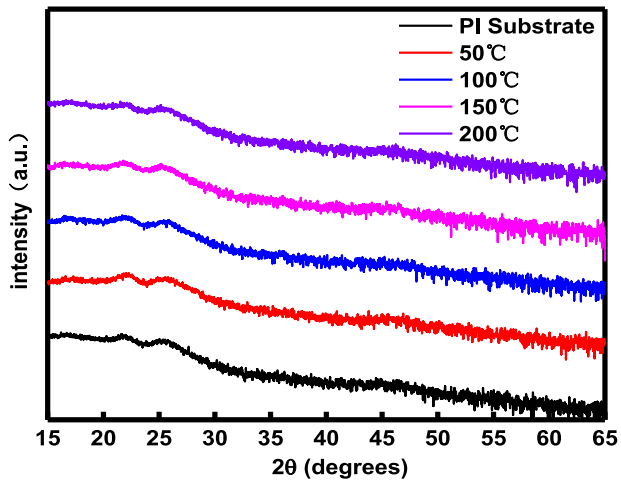

Fig. 2. X-ray diffraction patterns of the sputtered Ga_2O_3 films deposited under different temperatures.

electron microscope (FE-SEM, S-1400 Hitachi). The electrical characterizations were measured by Keithley 4200 semiconductor parameter analyzer. The I–V and time-dependent photoresponse tests under illumination were performed using a low pressure mercury lamp with 254 nm and 365 nm UV light.

3. Results and Discussion

Fig. 2 shows the X-ray diffraction (XRD) patterns of the films grown at different growth temperatures. All the patterns are the same with that of the PI substrate and there is no obvious peaks are observed, showing an amorphous state. In fact, the films grown on the rigid substrates (sapphire, quartz) at 200 °C are also amorphous as Fig. S1 shows, indicating that under such a low growth temperature range (50 °C to 200 °C) the crystal Ga_2O_3 cannot be formed no matter what the substrate is. The SEM images for the films grown at different temperatures are shown in Fig. S2, and the surface morphologies of the films grown at various temperatures are not much different, corresponding to the same amorphous state obtained by the XRD measurement.

Fig. 3 shows the ultraviolet-visible transmittance spectrum (200–800 nm) of the films grown at 200 °C. It can be observed that the Ga_2O_3 film on the PI substrate shows a cutoff absorption wavelength between 500 nm and 600 nm, and it is obviously not corresponding to the Ga_2O_3 material with a bandgap near 5.0 eV. To confirm this, the transmittance spectra of Ga_2O_3 films on the PI substrates grown at different temperatures and the pure PI substrate are measured and shown in the Fig. S3. It is demonstrated that the films on the PI substrates grown at different

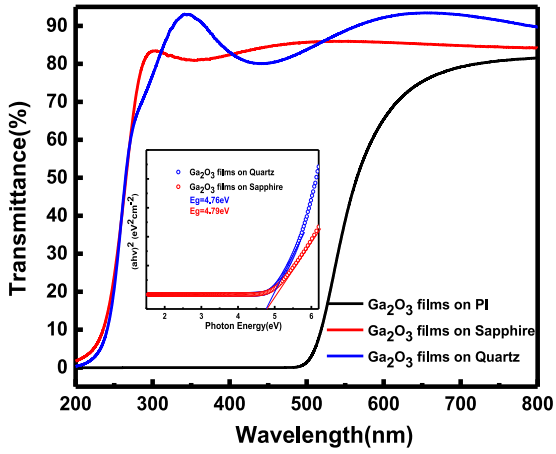

Fig. 3. Optical transmittance and the plot of $(\alpha h\nu)^2$-$h\nu$ in inset.

TABLE 1
Electrical parameters of photodetectors under different deposition temperatures

Deposition temperature(°C)	Optical responsivity(A/W)	External quantum efficiency(EQE)(%)	Photo-to-dark current ratio	UV-C to UV-A rejection ratio	τ_d (s)
50	1.2	575	397	60	0.27
100	2.2	1078	7400	2400	0.33
150	22	11000	5700	634	0.25
200	52.6	26000	230000	27000	0.38

temperatures show similar optical transmittance characteristics with the PI substrate, indicating that the transmittance of the films grown at each temperature is dominated by the PI substrate due to its optical absorption in the visible light band. So for further characterization of the optical characteristics of the Ga_2O_3 material itself, we studied the transmittance of Ga_2O_3 thin films grown on quartz and sapphire substrates as shown in Fig. 3 since it has been proved that the films at all these substrates are all amorphous from the XRD test and the material growth is not selective to substrate. When the incident light wavelength is less than 254 nm, the films have a strong absorption to UV light. And we have found that Ga_2O_3 films on sapphire substrate have an average transmittance of more than 80% in the visible light region (The transmittance of Ga_2O_3 films on quartz substrates is even more than 90%. And fluctuations in the visible light range are caused by optical interference effects.). The absorption edge of the samples is obtained from $(\alpha h\nu)^2$-$h\nu$ plots as shown in the inset in Fig. 3, where α is the absorption coefficient and $h\nu$ is the photon energy. The bandgap of all films is about 4.8 eV, which is similar to the reported values [19]–[21].

Fig. 4(a) presents the I–V characteristics of the flexible Ga_2O_3 UV photodetectors grown at different growth temperatures under the 254 nm UV illumination. Our UV light possesses power densities of 200 $\mu W/cm^2$. It can be seen that the Ti/Au electrodes show an Ohmic-type contact. As Ga_2O_3 film growth temperature increases, the current increases significantly. At 200 °C, the current reaches 396 nA at 20 V (corresponding responsivity is 52.6 A/W, and the external quantum efficiency is 2.6 $\times$ 10^4%). It has the highest values of optical responsivity and external quantum efficiency under all deposition temperatures as shown in Table 1. Fig. 4(b) and (c) show the I-V characteristics of the photodetectors under different wavelength irradiation for the growth temperature of 200 °C in linear and logarithmic coordinate respectively (Fig. S4 shows all devices' characteristics under other growth temperature). The dark current is as small as 1.7 pA at 20 V, and corresponding

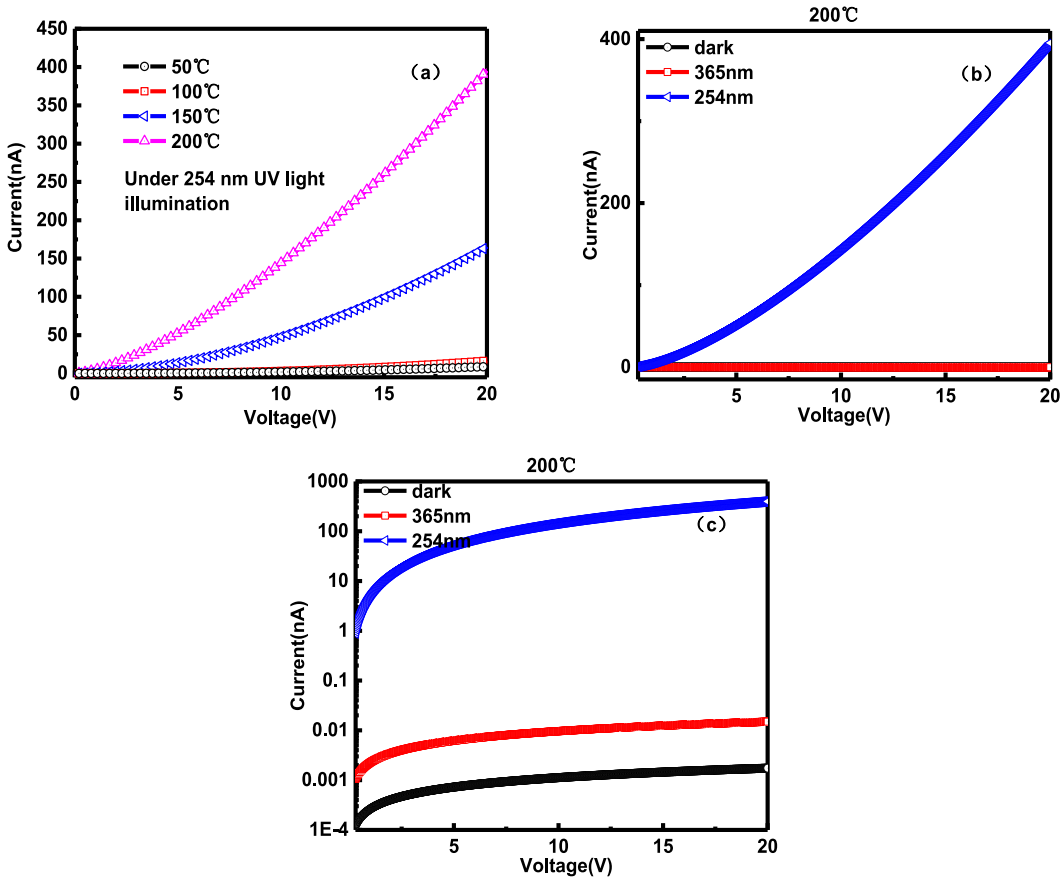

Fig. 4. (a) The current voltage (I-V) characteristics of Ga_2O_3 photodetectors grown at different deposition temperatures under 254 nm illumination, (b) the current-voltage (I-V) characteristics of the Ga_2O_3 films deposited under 200 °C in dark, 254 nm and 365 nm, and (c) its log scale.

photo-to-dark current ratio is more than 10^5. The photocurrent is 14.9 pA under 365 nm irradiation, which is slightly larger than the dark current. The reason for the response under 365 nm irradiation is that the film grown on the flexible material still have some defects. The UV-C to UV-A rejection ratio (254 nm versus 365 nm) reaches 2.7×10^4, which is far greater than the values at other temperatures as shown in Table 1, indicating that the device has good characteristics to detect UV blind light.

To further investigate the electrical performance of flexible photodetectors at different growth temperatures, we also performed a transient time response test at 20 V bias, as shown in Fig. 5(a), all devices have good electrical stability to DUV periodic illumination. After multiple illumination cycles, the photocurrent of the photodetectors remains basically unchanged. However, it can be seen from Table 1 that the response time of the photodetector is slightly longer at 200 °C. This phenomenon can be explained from the XPS test results, as shown in the Fig. S5: the material has largest number of oxygen vacancies at 200 °C (The integration areas of the curve of oxygen vacancy are 62147.46, 63524.89, 56853.11 and 68406.74 for samples deposed at 50 °C, 100 °C, 150 °C and 200 °C, respectively.), so the charge trapping caused by the oxygen vacancies could be a lot, which makes the recovery time of the device slightly longer. At the same time, we conducted a variable voltage test with a photodetector at 200 °C as an example, and found that the device has good electrical repeatability under different bias as shown in Fig. 5(b).

In order to compare the electrical properties of the flexible and rigid photodetectors, we have also grown the film on a sapphire substrate at 200 °C and fabricated the photodetector. All growth

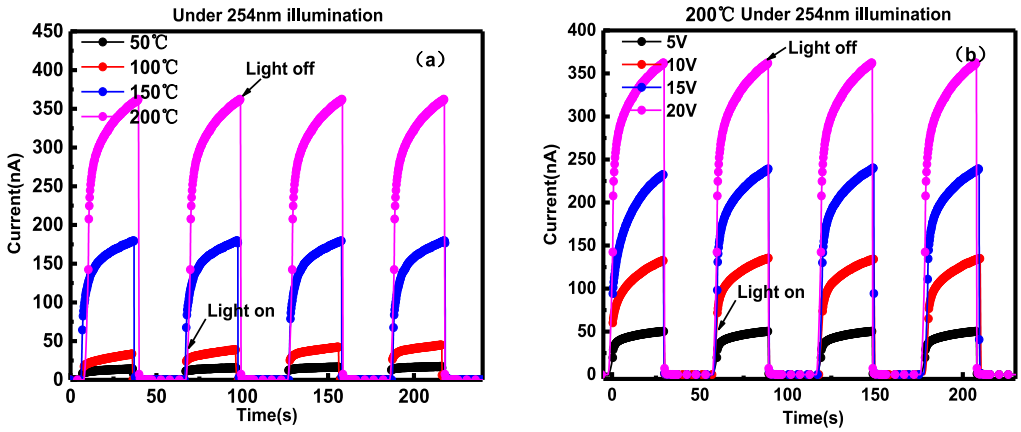

Fig. 5. Time-dependent photoresponse of the Ga_2O_3 flexible photodetector to 254 nm UV light illumination: (a) under different growth temperature at an applied bias of 20 V and (b) at different applied bias for growth temperature of 200 °C.

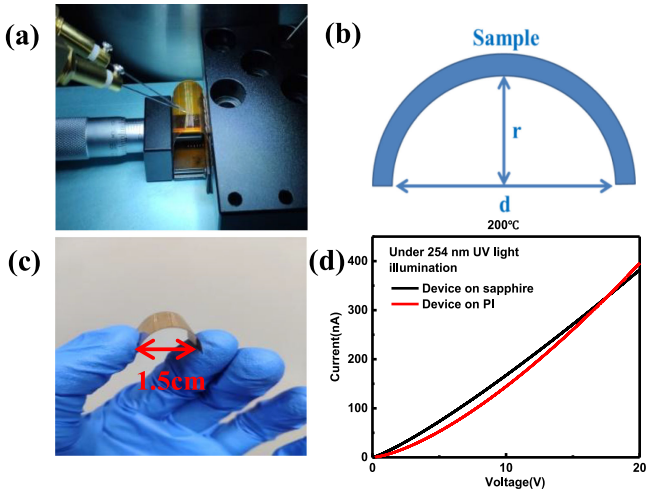

Fig. 6. (a) The image of the flexible photodetector fixed on a probe station. (b) The digital photographs of the flexible photodetectors. (c) Schematic diagram of bending diameter = d. (d) Performance comparison of the photodetectors on sapphire and PI substrate.

parameters were the same as those on the flexible substrate. As shown in Fig. 6(d), the photodetector on the flexible PI substrate exhibits similar electrical characteristics with the photodetector on the rigid sapphire substrate, which also shows that the flexible photodetector has good electrical properties. However, the electrical characteristics of the flexible photodetector show that it is not so good Ohmic-type contact as that for the rigid photodetector. This nonideal Ohmic contact property is supposed to from the mechanical properties and chemical properties of the flexible substrate, which results in the weak adhesion between the electrode and the material. This situation can be solved by inserting an intermediate adhesion layer, which will be our future work.

The most important aspect of flexible devices is the characterization of mechanical properties, which are the effects of bending and fatigue testing on the device performance. At the same time, for wearable devices, durability under bending conditions is essential [23]–[25]. Fig. 6(a) shows the image of the flexible photodetector fixed on a probe station. Fig. 6(b) shows the schematic diagram of bending diameter = d. Fig. 6(c) shows the digital photographs of the flexible photodetectors. The specific tests are the photocurrent–voltage curves, time response and fatigue test of the devices

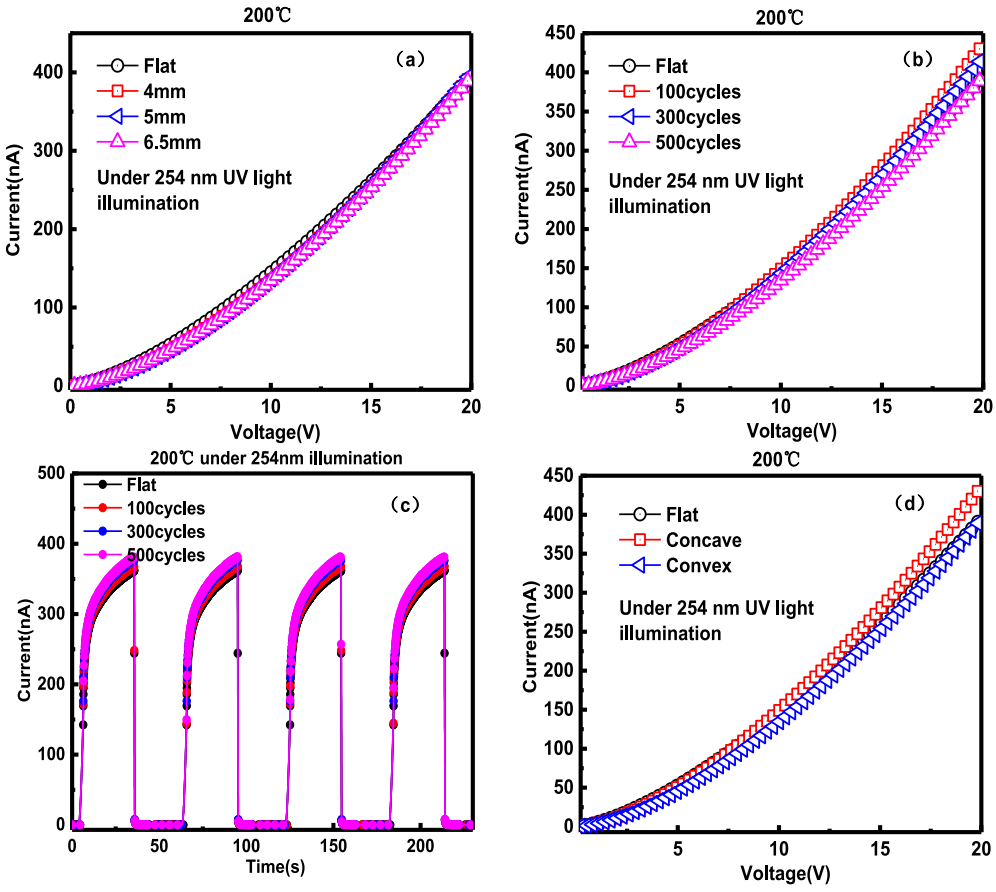

Fig. 7. (a) Bending test (r = 4, 5, 6.5 mm), (b) and (c) fatigue test, and (d) concave and convex test curve.

under different bending diameters. We take the photodetector at 200 °C as an example. The devices at other temperatures are described in the supporting file (Fig. S6, Fig. S7, Fig. S8). The curved device has a bending diameter d, as shown in Fig. 6(b), and the bending diameter d represents the degree of bending. First, we tested the photoresponse performance of the photodetector under different bending diameters. As shown in Fig. 7(a), the flexible photodetector exhibits similar electrical characteristics under curved state as in the flat state, indicating the bending of the photodetector has weak impact on performance of the photodetector, and flexible photodetectors exhibit good mechanical properties. However, it can be seen from the Fig. S9 that when the bending diameter is further reduced, the electrical properties of the photodetector begin to decline, indicating that the flexible device can exhibit stable electrical characteristics only within a certain bending range. Fig. 7(b) shows the current-voltage curve of the flexible photodetector at a curvature degree r = 4 mm after multiple bendings. We found that the photodetectors still showed the same curve even after 500 cycles bending fatigue tests. Fig. 7(c) shows the time response curve measured after multiple bendings, indicating that the flexible photodetector has very good electrical stability. It can be seen from the Fig. S6 and Fig. S7: at the growth temperature of 50 °C and 100 °C, the photodetectors have a current accumulation effect, that is, the current of each illumination period is larger than the current of the previous illumination period. However, at the growth temperature of 150 °C and 200 °C, the photodetectors exhibit good characteristics. Finally, as shown in Fig. 7(d), After the concave and convex test, the photodetector still exhibits the same electrical characteristics as the flat state, further illustrating the flexible Ga_2O_3 photodetector has good robustness and satisfying flexibility.

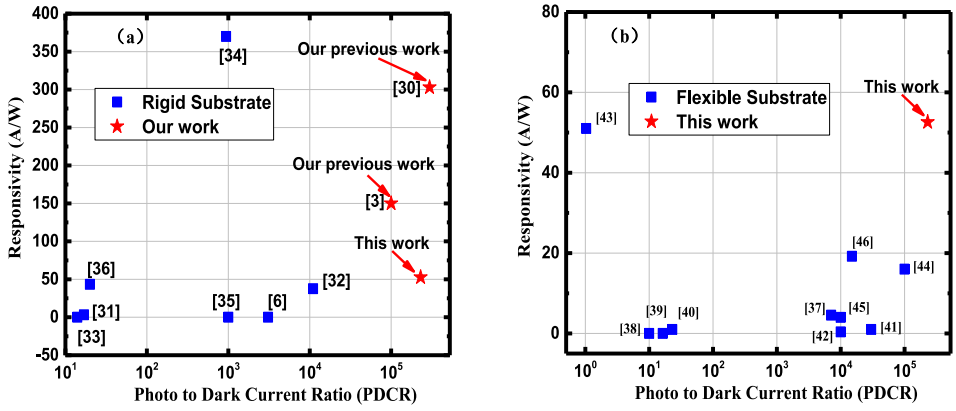

Fig. 8. Performance comparison of our solar blind Ga_2O_3 UV flexible photodetector with previously reported ones (the reference numbers are shown in brackets) for photo to dark current ratio and responsivity.

Responsivity and photo-to-dark current ratio are important indicators for evaluating the electrical performance of the photodetector. As shown in the Fig. 8, by quantitative comparison with the performance of the photodetectors in other papers, we can find that the our flexible photodetector shows a large photo-to-dark current ratio and responsivity, which is better than most MSM-structured photodetectors and is among the best reported Ga_2O_3 UV photodetectors.

4. Conclusion

In summary, the amorphous Ga_2O_3 films were successfully grown on a flexible PI substrate by RF magnetron sputtering at different growth temperatures. When the incident light wavelength is less than 254 nm, the incident light is absolutely absorbed by Ga_2O_3 films. The electrical results show that the flexible photodetectors exhibit good durability and stability at all growth temperatures on the one hand; on the other hand, the photodetector has the largest photo-to-dark current ratio ($>10^5$), responsivity (52.6 A/W), external quantum efficiency (2.6×10^4%) at 200 °C.

References

[1] R. Köhler *et al.*, "Terahertz semiconductor-heterostructure laser," *Nature*, vol. 417, pp. 156–159, 2002.
[2] X. Fan *et al.*, "Nonpolar and semipolar ultraviolet multiple quantum wells on GaN/sapphire," *Mater. Sci. Semicond. Process.*, vol. 92, pp. 103–107, 2019.
[3] Y. Xu *et al.*, "Solar blind deep ultraviolet β-Ga_2O_3 photodetectors grown on sapphire by the mist-CVD method," *Opt. Mater. Exp.*, vol. 8, pp. 2941–2947, 2018.
[4] D. Chen *et al.*, "Simulation study toward high-performance transparent-conductive-oxide free perovskite solar cells using metal microcavity and optical coupling layer," *IEEE Photon. J.*, vol. 10, no. 2, Apr. 2018, Art. no. 8400209.
[5] K.-X. Sun, "Applications of robust, radiation hard AlGaN optoelectronic devices in space exploration and high energy density physics," in *Proc. Laser Sci. Photon. Appl.*, 2011, pp. 1–2.
[6] P. Feng, J. Zhang, Q. Li, and T. Wang, "Individual β-Ga_2O_3 nanowires as solar-blind photodetectors," *Appl. Phys. Lett.*, vol. 88, 2006, Art. no. 153107.
[7] M. Y. Liao and K. Yasuo, "High-performance metal-semiconductor-metal deep-ultraviolet photodetectors based on homoepitaxial diamond thin film," *Appl. Phys. Lett.*, vol. 89, 2006, Art. no. 113509.
[8] T. Oshima, T. Okuno, and S. Fujita, "Ga_2O_3 thin film growth on c-plane sapphire substrates by molecular beam epitaxy for deep-ultraviolet photodetectors," *Jpn. J. Appl. Phys.*, vol. 46, pp. 7217–7220, 2007.
[9] A. Rajan *et al.*, "Sol–gel derived Ag-doped ZnO thin film for UV photodetector with enhanced response," *J. Mater. Sci.*, vol. 48, pp. 7994–8002, 2013.
[10] A. Manekkathodi *et al.*, "Direct growth of aligned zinc oxide nanorods on paper substrates for low-cost flexible electronics," *Adv. Mater.*, vol. 22, pp. 4059–4063, 2010.
[11] P. Docampo *et al.*, "Efficient organometal trihalide perovskite planar-heterojunction solar cells on flexible polymer substrates," *Nature Commun.*, vol. 4, 2013, Art. no. 2761.

[12] X. Hou *et al.*, "SnO_2-microtube-assembled cloth for fully flexible self-powered photodetector nanosystems," *Nanoscale*, vol. 5, pp. 7831–7837, 2013.
[13] X. Chen *et al.*, "A self-powered solar-blind photodetector with fast response based on Au/β-Ga_2O_3 nanowires array film Schottky junction," *ACS Appl. Mater. Interfaces*, vol. 8, pp. 4185–4191, 2016.
[14] M. Orita *et al.*, "Deep-ultraviolet transparent conductive β-Ga_2O_3 thin films," *Appl. Phys. Lett.*, vol. 77, pp. 4166–4168, 2000.
[15] X. Lu. *et al.*, "Schottky x-ray detectors based on a bulk β-Ga_2O_3 substrate," *Appl. Phys. Lett.*, vol. 112, 2018, Art. no. 103502.
[16] D. Zhang, W. Zheng, R. C. Lin, T. T. Li, Z. J. Zhang, and F. Huang, "High quality β-Ga_2O_3 film grown with N_2O for high sensitivity solar-blind-ultraviolet photodetector with fast response speed," *J. Alloy Compd.*, vol. 735, pp. 150–154, 2018.
[17] X. Du *et al.*, "Preparation and characterization of Sn-doped β-Ga_2O_3 homoepitaxial films by MOCVD," *J. Mater. Sci.*, vol. 50, pp. 3252–3257, 2015.
[18] T. Oshima *et al.*, "β-Ga_2O_3-based metal–oxide–semiconductor photodiodes with HfO_2 as oxide," *Appl. Phys. Exp.*, vol. 11, 2018, Art. no. 112202.
[19] X. Wang *et al.*, "Optimizing the performance of a beta-Ga_2O_3 solar-blind UV photodetector by compromising between photoabsorption and electric field distribution," *Opt. Mater. Exp.*, vol. 8, pp. 2918–2927, 2018.
[20] T. T. Nang, M. Okuda, T. Matsushita, S. Yohota, and A. Suzuki, "Electrical and optical properties of Ge_xSe_{1-x} amorphous thin films," *Jpn. J. Appl. Phys.*, vol. 15, pp. 849–853, 1976.
[21] D. Guo *et al.*, "Fabrication of β-Ga_2O_3 thin films and solar-blind photodetectors by laser MBE technology," *Opt. Mater. Exp.*, vol. 4, pp. 1067–1076, 2014.
[22] S. H. Lee *et al.*, "High-responsivity deep-ultraviolet-selective photodetectors using ultrathin gallium oxide films," *ACS Photon.*, vol. 4, pp. 2937–2943, 2017.
[23] Y. S. Rim *et al.*, "Ultrahigh and broad spectral photodetectivity of an organic-inorganic hybrid phototransistor for flexible electronics," *Adv. Mater.*, vol. 27, pp. 6885–6891, 2015.
[24] M. Kataria *et al.*, "Transparent, wearable, broad band, and highly sensitive upconversion nanoparticles and graphene based hybrid photodetectors," *ACS Photon.*, vol. 5, pp. 2336–2347, 2018.
[25] B. Jerez *et al.*, "Flexible electro-optic, single-crystal difference frequency generation architecture for ultrafast mid-infrared dual-comb spectroscopy," *ACS Photon.*, vol. 5, pp. 2348–2353, 2018.
[26] K. Arora *et al.*, "Ultra-high-performance of self-powered β-Ga_2O_3 thin film solar-blind photodetector grown on cost-effective Si substrate using high-temperature seed layer," *ACS Photon.*, vol. 5, pp. 2391–2401, 2018.
[27] B. Zhao *et al.*, "Solar-blind avalanche photodetector based on single ZnO-Ga_2O_3 core-shell microwire," *Nano Lett.*, vol. 15, pp. 3988–3993, 2015.
[28] D. Guo, H. Liu, P. Li, and Z. Wu, "Zero-power-consumption solar-blind photodetector based on β-Ga_2O_3/NSTO hetero-junction," *ACS Appl. Mater. Interfaces*, vol. 9, pp. 1619–1628, 2017.
[29] Z. Ranran *et al.*, "A self-powered solar-blind photodetector based on a MoS_2/β-Ga_2O_3 heterojunction," *J. Mater. Chem. C*, vol. 6, pp. 10982–10986, 2018.
[30] Z. Li *et al.*, "Improving the production of high-performance solar-blind β-Ga_2O_3 photodetectors by controlling the growth pressure," *J. Mater. Sci.*, vol. 54, pp. 10335–10345, 2019.
[31] T. Oshima, T. Okuno, N. Arai, N. Suzuki, S. Ohira, and S. Fujita, "Vertical solar-blind deep-ultraviolet Schottky photodetectors based on β-Ga_2O_3 substrates," *Appl. Phys. Exp.*, vol. 1, 2008, Art. no. 011202.
[32] K. Sasaki, A. Kuramata, T. Masui, E. G. Villora, K. Shimamura, and S. Yamakoshi, "Device-quality β-Ga_2O_3 epitaxial films fabricated by ozone molecular beam epitaxy," *Appl. Phys. Exp.*, vol. 5, 2012, Art. no. 035502.
[33] R. Suzuki, S. Nakagomi, and Y. Kokubun, "Solar-blind photodiodes composed of an Au Schottky contact and a β-Ga_2O_3 single crystal with a high resistivity cap layer," *Appl. Phys. Lett.*, vol. 98, 2011, Art. no. 131114.
[34] W. Y. Weng, T. J. Hsueh, S. J. Chang, G. J. Huang, and H. T. Hsueh, "A β-Ga_2O_3/GaN hetero-structured solar-blind and visible-blind dual-band photodetector," *IEEE Sens. J.*, vol. 11, no. 6, pp. 1491–1492, Jun. 2011.
[35] X. Deng *et al.*, "Effect of processing parameters on the structural, electrical and magnetic properties of BFO thin film synthesized via RF magnetron sputtering," *J. Alloy Compd.*, vol. 684, pp. 510–515, 2016.
[36] Z. Zhang, Y. Tang, J. Chen, and J. Chen, "Influence of low sputtering pressure on structural, electrical and optical properties of Al-doped zinc oxide thin films," *Physica B*, vol. 495, pp. 76–81, 2016.
[37] M. Peng *et al.*, "High-performance flexible and broadband photodetectors based on PbS quantum dots/ZnO nanoparticles heterostructure," *Sci. China-Mater.*, vol. 62, pp. 225–235, 2019.
[38] K. Kwak, K. Cho, and S. Kim, "Flexible photodiodes constructed with CdTe nanoparticle thin films and single ZnO nanowires on plastics," *Nanotechnology*, vol. 22, 2011, Art. no. 415204.
[39] J. He *et al.*, "Synergetic effect of silver nanocrystals applied in PbS colloidal quantum dots for high-performance infrared photodetectors," *ACS Photon.*, vol. 1, pp. 936–943, 2014.
[40] S. Park *et al.*, "Significant enhancement of infrared photodetector sensitivity using a semiconducting single-walled carbon nanotube/C_{60} phototransistor," *Adv. Mater.*, vol. 27, pp. 759–765, 2015.
[41] Z. Zheng *et al.*, "Photodetectors: A fully transparent and flexible ultraviolet-visible photodetector based on controlled electrospun ZnO-CdO heterojunction nanofiber arrays," *Adv. Funct. Mater.*, vol. 25, pp. 5877–5877, 2015.
[42] S. Lim *et al.*, "Broadband omnidirectional light detection in flexible and hierarchical ZnO/Si heterojunction photodiodes," *Nano Res.*, vol. 10, pp. 22–36, 2017.
[43] Y. Liu *et al.*, "Graphene-carbon nanotube hybrid films for high-performance flexible photodetectors," *Nano Res.*, vol. 10, pp. 1880–1887, 2016.
[44] D. B. Velusamy *et al.*, "Flexible transition metal dichalcogenide nanosheets for band-selective photodetection," *Nature Commun.*, vol. 6, 2015, Art. no. 8063.
[45] D. B. Velusamy *et al.*, "2D organic-inorganic hybrid thin films for flexible UV-visible photodetectors," *Adv. Funct. Mater.*, vol. 27, 2017, Art. no. 1605554.
[46] P. A. Hu *et al.*, "Highly responsive ultrathin GaS nanosheet photodetectors on rigid and flexible substrates," *Nano Lett.*, vol. 13, pp. 1649–1654, 2013.